(Article begins on next page)

Phase Noise Impact in Self-homodyne short-reach coherent transmission using DFB lasers

Giuseppe Rizzelli, Antonino Nespola, Stefano Straullu, Fabrizio Forghieri and Roberto Gaudino, *Senior Member, IEEE*

***Abstract*—We investigate on a two-fiber short-reach self-homodyne coherent transmission system without optical amplification, where the same transmission laser is used to generate a modulated signal carrying useful data and a continuous wave signal, which serves as a local oscillator at the receiver side. Target of the work is to determine by experiments and theoretical models under which conditions DFB lasers can be used instead of more expensive ECL lasers. After careful characterization of lasers phase noise in terms of linewidth as a function of the mismatch between the optical paths of the signal and of the local oscillator, the performance of two laser technologies is investigated in the proposed transmission setup, showing that commercial DFB laser can be used, provided that the optical path mismatch between the two fibers is kept below 1.8 meter for 28 $GBaud$ PM-QPSK and 0.8 meter for PM-16QAM modulation format in combination with a soft-decision forward error correction algorithm. After an experimental demonstration, we theoretically investigate the scalability laws of the proposed systems in different configuration flavours.**

***Index Terms*—Coherent Detection, Optical Fiber Communication, Passive Optical Networks.**

I. Introduction

In recent years, coherent detection (Coh-D) has enabled an unprecedented capacity increase to multi-Terabit in long-haul optical transmission [1], [2], progressively replacing traditional systems based on intensity modulation and direct detection (IM-DD). In spite of the fact that more than 90% of the generated data is exchanged within or among data centers (DCs), short-reach networks ($<10\ km$) still mainly rely on Intensity Modulation and Direct Detection (IM-DD) solutions due to the additional cost and complexity constraints associated with Coh-D and advanced modulation formats. However, the research and industry community is actively working toward a transition from IM-DD to Coh-D in the medium term, since DCs are facing the challenge to upgrade their capacity per wavelength beyond 100 $Gb/s/\lambda$ to support the growing traffic demand. It seems unlikely that current IM-DD solutions will be able to ensure capacities beyond 200 $Gb/s/\lambda$ in the mid- to long- term [3], [4]. Thus, industry organizations such as the Optical Internetworking Forum (OIF) and the IEEE have initiated Coh-D standardization activities [5], reinforcing the view of coherent communication moving to shorter reach, high volume applications.

G. Rizzelli and R. Gaudino are with the Department of Electronics and Telecommunications, Politecnico di Torino, Torino, Italy, e-mail: giuseppe.rizzelli@polito.it.

A. Nespola and S. Straullu are with LINKS Foundation, Torino, Italy.

F. Forghieri is with CISCO Photonics Italy, Vimercate, Italy.

Although, as we show in [6], [7], Coh-D can in principle provide remarkable power budgets even at extremely high bit rates and without optical amplification, to date cost factors have prevented it from being extensively employed in short reach scenarios [8], [9]. Considering Silicon Photonics optoelectronic platforms, one of the most promising low cost solutions for DC applications, almost all optoelectronic components required by a coherent system can today be integrated with the only (but cost-wise fundamental) exception of the laser, that in Coh-D has much stringent specs compared to IM-DD, usually requiring External Cavity Lasers (ECL) that up to now cannot be integrated directly [10] but requires hybrid integration with another semiconductor platform. Thus, several recent papers have proposed system-level solutions to use simpler lasers, and in particular uncooled Distributed Feedback (DFB) lasers (which would be significantly less expensive than ECL), resorting to novel two-fiber self-homodyne systems [8], [11], [12], where the transmitted signal is split prior to modulation and the continuous wave (CW) portion is sent on one fiber, whereas the modulated portion propagates along another fiber inside the same cable. At the Coh-D receiver, the CW signal is used as LO as shown in Fig. 1.

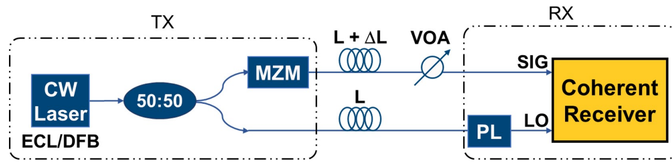

Fig. 1: Experimental setup of the self-coherent transmission system. DFB: Distributed Feedback Laser; ECL: External Cavity Laser; MZM: Mach Zhender Modulator; VOA: Variable Optical Attenuator; SIG: Signal; LO: Local Oscillator, PL: Polarization Locker.

Differently from the traditional intradyne coherent detection, self-homodyne detection requires the LO state of polarization to be tracked in order to compensate for random polarization rotations along the propagation distance. Many works have addressed this issue by employing integrated optical polarization controllers [13]–[15] with insertion losses as low as 2 dB.

In this paper, we extend the analysis of [8], [12], [16] by experimentally investigating on the use of commercial DFB lasers as a low-cost alternative to narrow linewidth ECL. We also complement the theoretical analysis presented in [11] by experimentally characterizing the laser phase noise in a self-coherent system. As a main result of our paper, we show that this self-homodyne approach enables the use of commercial DFB lasers provided that the path difference between the two fibers is below 0.8 meter for PM-16QAM and 1.8 meter for PM-QPSK (both at 28 $GBaud$).

We believe that this architecture is very interesting for intra-data center (IDC), for instance in scenarios using multi-parallel optic (MPO) cable, where the "waste" of one fiber for the LO could be accepted when considering the increase in bit rate enabled by Coh-D compared to a traditional IM-DD solution. In fact, as an extension of our previous work [16], after the experimental demonstration, the paper continues with a theoretical scalability study, showing potential evolution towards higher baud rate and different system architectures.

The paper is organized as follows. In Section II, we experimentally characterize the resulting beating linewidth for the self-coherent system using a commercial DFB laser at the transmitter, showing that it decreases when the difference in length between the two path decreases. The experimental results are then compared to a numerical model, showing a good agreement. In Section III we then introduce the actual experiment, showing back-to-back (B2B) system performance as a function of the path difference, showing a 1 dB sensitivity penalty at about 1.8 m and 0.8 m path difference for polarization multiplexed- (PM-) QPSK and PM-16QAM modulation, respectively, at BER=$2 \cdot 10^{-2}$. We also present transmission results in a realistic IDC scenario showing that no penalty is introduced by a 2.5 km fiber optic link with respect to the back-to-back condition, and we show the effect of phase noise on the phase recovery stage of the DSP. In Section IV we then introduce a numerical model to study the scalability of the system towards higher bit rates and different architectures, and in particular we discuss on the resulting power budget and sensitivity margin of systems based on a multi-parallel optic (MPO) cable, where one optical fiber is dedicated to transporting the CW signal to be used as LO at the receiver, and the others for several modulated streams in parallel. We conclude in Section V with some final comments and remarks.

II. Laser Linewidth in Self-Coherent Beating

The two-fiber self-coherent setup shown in Fig. 1 is, apart from the modulation, identical to the well-known coherent delayed self-heterodyne (CDSH) method [17] for laser linewidth characterization. In fact, we start our work by measuring the resulting beating linewidth in this specific situation, since this is the fundamental parameter for phase noise impact in coherent transmission systems, requiring sufficiently narrow linewidth in order to keep phase noise impairments under control as discussed in the next section. In particular, we focus on the resulting beating linewidth when one signal travels along a fiber of length L, while the other propagates on another fiber with length $L + \Delta L$. We will show in this paper that ΔL (i.e. the path difference between the two arms) is a fundamental parameter in the proposed system. To avoid confusion, we remark that for our system we are interested in small ΔL, as we will show later, while normally the CDSH method introduces a very large ΔL to obtain full decorrelation between the two beating signals.

In order to register the resulting beating using the AC-coupled optoelectronic available in our lab, in the experiment one of the two signals is frequency shifted (by f_{AOM} =27 MHz) using an acousto-optic modulator (AOM). The beating linewidth measurements were performed on 1550 nm commercial lasers (an ECL taken as a benchmark and a DFB whose specsheets indicate a <100 kHz and <10 MHz nominal linewidth, respectively) for ΔL ranging from 0 m to 5 m. Precise estimation of the path difference was obtained by sending a 0.1 ns pulse on the two arms and measuring the time delay between the two at the input of the coherent receiver (CR) by means of a PIN photodector and an oscilloscope. The beat-signal (that in the electrical spectrum is placed around f_{AOM}), was acquired through a real-time oscilloscope, then the resulting spectrum was estimated via FFT. Fig. 2a and

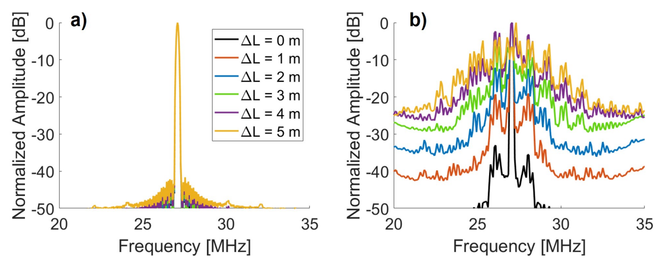

Fig. 2: Measured power spectral density with 100 kHz RBW of a) an ECL laser and b) a DFB laser for different path differences ΔL. Legend in a) applies to b) as well.

Fig. 2b show the normalized power spectral density with 100 kHz resolution bandwidth (RBW) of the ECL and the DFB laser for different path differences ΔL. As expected, the ECL beating spectrum remains unaffected for all the considered values of ΔL, since the path mismatches are much shorter than its coherence length (which can be estimated to be 2.1 km given the nominal 100 kHz linewidth). On the contrary, the DFB beating spectrum, shows much larger frequency contributions spanning a frequency range around the central frequency that increases significantly with the path difference, yielding an overall larger linewidth. Fig. 2b shows that the DFB self-beating linewidth (SBL) can be reduced by keeping ΔL sufficiently short, as indicated even more evidently in Fig. 3 where a 1 MHz RBW was used.

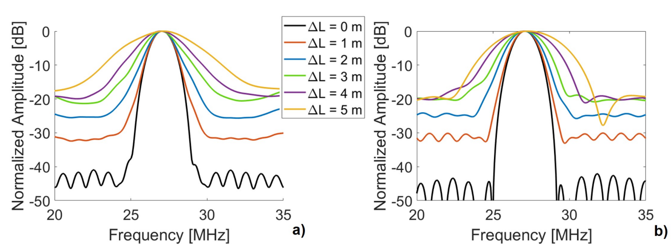

Fig. 3: a) Measured power spectral density with 1 MHz RBW of a DFB laser and b) fitted power spectral density of a DFB laser for different path differences ΔL simulated solving the numerical model presented in [18].

This anticipates that the phase noise penalty that affects Coh-D systems when using DFB could be reduced by decreas-

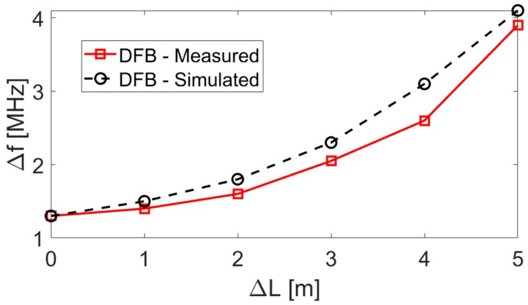

Fig. 4: Measured (solid red line) and numerically simulated (dashed black line) 3dB linewidth Δf as a function of the path differences ΔL for DFB (red, squares) laser. The RBW is 1 MHz, which limits the minimum obtainable Δf.

ing ΔL, as we will confirm in the transmission experiments in the next Section 3. Intuitively, the linewidth (or phase noise) reduction for decreasing ΔL can be easily interpreted at the limit of ΔL=0. In this case, independently on the instantaneous value assumed by phase noise, the two signals reaching the photodiode (or the coherent receiver in the following Section III) have exactly the same phase, so the beating is always perfectly in phase, resulting in an extremely narrow beating linewidth. A numerical confirmation of this physical phenomenon was obtained through the fitting of the experimental results shown in Fig. 3a with the model presented in [18]. For space limitations we do not report it here, but we follow exactly equation (17) in [18] where an expression for the frequency noise spectrum was derived taking into account both the white frequency noise and the $1/f$ noise, and showed that the contribution of the latter to the delayed self-heterodyne linewidth measurement comprises a broad base and a narrow spike in the power spectrum of the laser for short time delays, and results in an additional broadening with respect to the natural Lorentzian linewidth for longer delays. Fig. 3b shows the simulated DFB laser spectra highlighting the same trends and an excellent agreement with the experiments in Fig. 3a for the same ΔL values. The fitting was carried out in the displayed [20,35] MHz frequency range and the resulting 3dB linewidths (Δf) are reported in Fig. 4 (dashed line) as a function of ΔL, for the DFB laser in comparison with the measured values (solid line), when the RBW is 1 MHz. Small discrepancies between measurements and numerically fitted values are attributable to the model being unable to perfectly reproduce all the spectral features over such a broad frequency range. It is worth mentioning that the RBW limits the minimum obtainable linewidth in Fig. 4 as well as in Fig. 2, where both the ECL and the DFB main lobe linewidths are likely much narrower then what the instrument resolution allows to measure.

III. Self-Coherent Transmission Experiments

A. Back-to-back

The self-coherent setup used in our experiments is shown in Fig. 1. The transmitted signal is split equally on two optical paths: one is modulated and represents the data-carrying traffic, whereas the other propagates untouched as a CW signal used as a LO oscillator at the Coh-D receiver. This scheme envisages the two signals propagating separately on two different fibers inside the same cable, for instance in IDC scenarios using MPO cable and where the waste of one fiber for the LO would certainly be compensated considering the increase in bit rate enabled by Coh-D compared to a traditional IM-DD solution.

We modulate the signal by an external Mach-Zehnder modulator (MZM) to generate PM-QPSK or PM-16QAM signals at 28 $Gbaud$. The MZM is driven by a 92 GS/s arbitrary waveform generator (AWG) working as a four output digital-to-analog converter, using off-line processing approach. The input digital streams are four independent PRBS15 sequences. After fiber transmission and attenuation, we used a commercial Coh-D receiver and a real time oscilloscope at 200 GS/s and post-processed the data after downsampling at two samples per symbol through typical off-line DSP routines for Coh-D systems. A detailed description of the used DSP can be found in Section IIIII-B. We characterize the system performance measuring BER vs. received optical power P_{RX}, varied at the CR input through a variable optical attenuator (VOA).

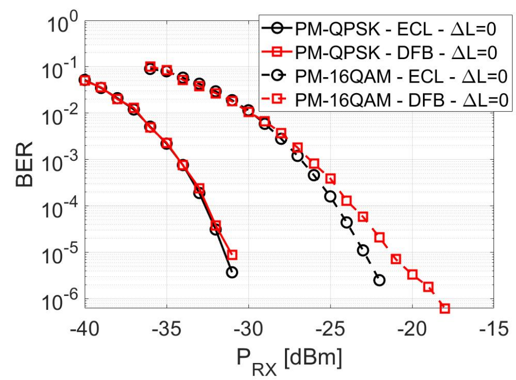

Fig. 5: Measured B2B sensitivity curves for 28 $GBaud$ PM-QPSK (solid lines) and 16-QAM (dashed lines) transmission with ECL (black, circles) and DFB (red, squares) laser for path difference ΔL=0.

As a system performance benchmark, Fig. 5 shows the self-coherent B2B sensitivity curves for the DFB- and ECL-based transmission of 28 $GBaud$ PM-QPSK and PM-16QAM modulated data when ΔL equals 0 m. The LO power at the input of the coherent receiver is 9 dBm. We observe that no significant penalty is present between the DFB and ECL cases, for both modulation formats and BER values above the $4 \cdot 10^{-3}$ hard-decision forward error correction (HD-FEC) threshold, showing that the DFB laser behaves exactly as the ECL laser in a self-coherent setup when ΔL is sufficiently small, with a sensitivity of about -36 dBm and -28 dBm for PM-QPSK and PM-16QAM, respectively. Below the HD-FEC threshold small deviations from the ECL-based system performance occur only for PM-16QAM modulation and DFB laser, with penalties greater than 1 dB only for low BER smaller than 10^{-4}.

We thus prosecute by studying the resulting performance when varying the difference ΔL between the two optical path lengths. Starting from PM-QPSK, Fig. 6a shows the B2B sensitivity curves for the DFB-based system with 28 $GBaud$ PM-QPSK modulation and for ΔL values from 0 m to 5 m, with 1 m step. As anticipated, the effect of phase noise induces a power penalty that increases with ΔL. In particular, Fig. 6b shows the evolution of the penalty vs. ΔL at two different BER levels: a $2 \cdot 10^{-2}$ soft-decision forward error correction (SD-FEC) threshold, and the $4 \cdot 10^{-3}$ HD-FEC threshold. The figure shows that the path difference should remain below 1.3 meter and 1.8 meter to have less than 1 dB penalty at the HD-FEC and SD-FEC threshold, respectively.

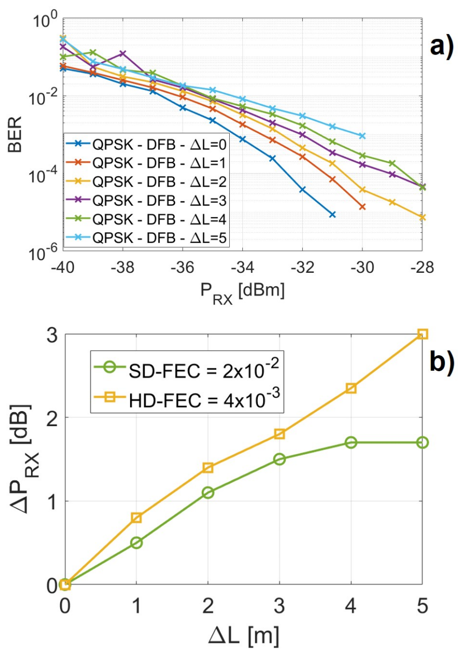

Fig. 6: a) B2B sensitivity curves for the DFB-based system with 28 $GBaud$ PM-QPSK modulation and for ΔL values from 0 m to 5 m. b) Received optical power penalty for SD-FEC BER threshold $2 \cdot 10^{-2}$ (green, circles) and HD-FEC BER threshold $4 \cdot 10^{-3}$ (orange, squares).

It is worth mentioning here that throughout the paper we compare performance at fixed baud rate, regardless of the FEC threshold. Therefore, the net bit rate would depend on the specific implementation of the FEC algorithm, which introduces an additional overhead. For 100 $Gbps$ transmission, for instance, 28 $GBaud$ are sufficient for HD-FEC with typical 7% overhead, whereas the baud rate should be increased when considering SD-FEC algorithms with higher overhead (typically 15-35%).

Fig. 7a and b show the same results for PM-16QAM modulation. In this case the tolerance to the optical path difference is further reduced to approximately 0.4 meter and 0.8 meter to ensure less than 1 dB penalty at the HD-FEC and SD-FEC threshold, respectively. This requirement does not seems exceedingly critical from a system point of view, when considering an integrated transceiver (where optical path difference can be controlled with very high accuracy) and, moreover, if the two fibers run along the same cable, such as in

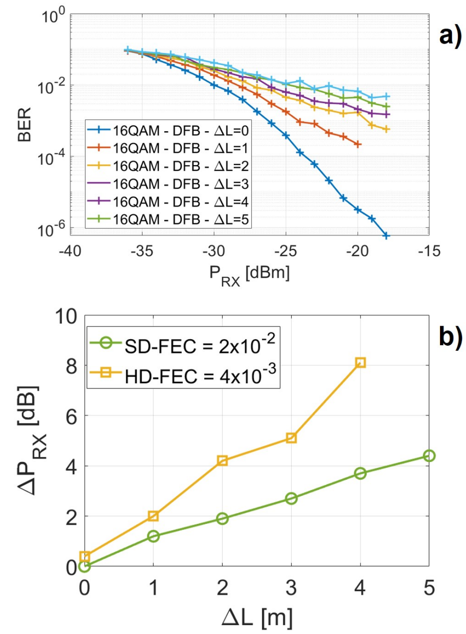

Fig. 7: a) B2B sensitivity curves for the DFB-based system with 28 $GBaud$ PM-16QAM modulation and for ΔL values from 0 m to 5 m. b) Received optical power penalty for SD-FEC BER threshold $2 \cdot 10^{-2}$ (green, circles) and HD-FEC BER threshold $4 \cdot 10^{-3}$ (orange, squares).

MPO cable. Furthermore, the tolerance to the path difference would be further increased at higher baud rates, as the impact of phase noise reduces with the data rate [19]–[21].

B. Short-reach Transmission Experiments

In a more realistic transmission experiment we included a 2.5 km standard SMF link in the setup shown in Fig. 1. Fig. 8 shows the sensitivity curves for the DFB-based PM-QPSK and PM-16QAM systems for 0 m and 1 m path difference. In this case, the correct SOP of the LO is ensured by a polarization locker (PL), similarly to what was proposed in [8] and [12], and implemented experimentally in [13], [14] with a Silicon Photonic integrated device. In our experiment we used a Thorlabs PL1000S SOP locker as a PL. As discussed in the final section of our paper, the need of a PL is the only true drawback of the proposed setup. Please note that this set of measurements was carried out at a different time than those presented in Fig. 6 and Fig. 7, therefore a slightly different setup may have affected the B2B sensitivity. Nevertheless it is worth noting that even in a realistic transmission scenario 0 m path difference is perfectly equivalent to B2B transmission, and that when ΔL=1 m the power penalty is again 0.5 dB at the SD-FEC threshold and 0.75 dB at the HD-FEC threshold for PM-QPSK modulation, as in Fig. 6. Also in the PM-16QAM case no significant difference was observed in realistic transmission over a 2.5 km link.

The results presented in Fig. 8 were obtained using a quite common DSP algorithm, such as the one presented in [22]: it is based on the use of a standard constant modulus algorithm (CMA) followed by a Viterbi-Viterbi stage for carrier-phase

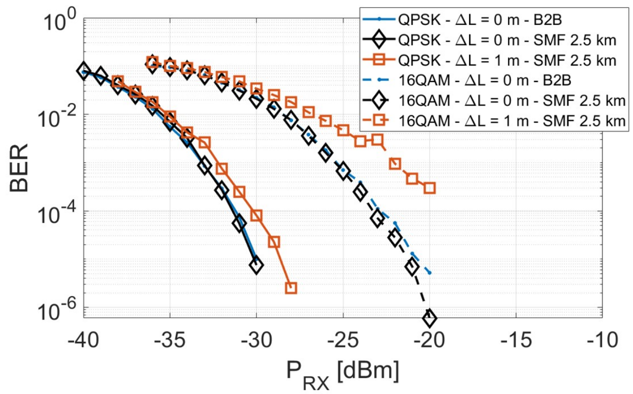

Fig. 8: Comparison of sensitivity curves in B2B and with a 2.5 km SMF link for 0 m and 1 m path difference for PM-QPSK (solid) and PM-16QAM (dashed) modulation formats.

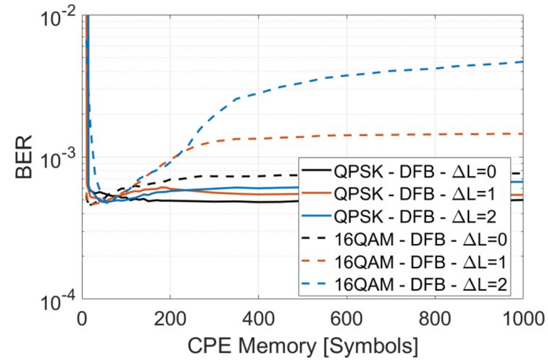

Fig. 9: BER as a function of the number of symbols used for carrier phase estimation for different values of the path difference ΔL and for 28 $GBaud$ PM-QPSK (solid lines) and PM-16QAM (dashed lines) modulation when DFB laser is used for signal generation.

estimation (CPE) over an optimized number of symbols. In a previous work [23] we found that standard coherent detection coupled with the use of DFB lasers requires careful optimization of the DSP parameters and, in particular, of the memory of the CPE. Thus, here we have investigated how the performance of the self-coherent solution is affected by this important parameter.

Fig. 9 shows the BER as a function of the number of symbols used in the CPE stage of the DSP for the two considered modulation formats and different ΔL values up to 2 meters when a DFB laser is used at the transmitter. For a fairer comparison, all the measurements have been performed by setting different received power levels for each case, so that all the curves have the same minimum. The actual received optical power level for the two modulation formats can be found from Fig. 8 at BER=$5 \cdot 10^{-4}$. The results highlight that the CPE memory impact on the PM-QPSK modulation is negligible for up to 1000 symbols, whereas PM-16QAM modulation is strongly affected for high (and unrealistic) CPE memory values above 200 symbols. However, the self-coherent system results to be quite robust to the laser phase noise at these optical path differences, allowing for a reasonable number of symbols (in the common range 30 to 50) to be used for phase recovery with negligible BER penalty.

IV. Theoretical Scalability Study

A. Analytical Model

Following the approach presented in [6], [7], we derived an analytical model for unamplified self-coherent receiver, based on the study first reported in [24] and confirmed in [25], [26], which we will use in the following Section IVIV-B to produce some general scalability laws for a proposed MPO-based system configuration.

A detailed description of the model can be found in [7]. It computes the equivalent signal-to-noise ratio (SNR) on each of the four output electrical signals (corresponding to each of the four available quadratures) of a coherent receiver, in terms of the relevant system parameters:

$$SNR_{RX} = \frac{P_s}{\dfrac{\sigma_{th}^2}{P_L^{CW}} + P_L^{CW} \cdot \sigma_{n_{LO}}^2 \cdot CMRR + \sigma_{shot}^2 + \dfrac{P_s}{SNR_Q}} \quad (1)$$

where P_s is the received modulated signal optical power, P_L^{CW} is the CW optical power of the local oscillator, $CMRR$ is the Common Mode Rejection Ratio of the balanced photodetector, $\sigma_{n_{LO}}^2$ is the variance of the LO RIN contribution, σ_{th}^2 is the variance of the TIA thermal noise and σ_{shot}^2 is the variance of the shot noise generated in the photodetection process. These three terms can be expressed as:

$$\sigma_{th}^2 = \frac{i_{TIA}^2 \cdot B_{eq}^{RX}}{8 \cdot R^2}; \quad \sigma_{shot}^2 = \frac{q \cdot B_{eq}^{RX}}{2 \cdot R}; \quad \sigma_{n_{LO}}^2 = RIN \cdot \frac{B_{eq}^{RX}}{2} \quad (2)$$

where R is the overall responsivity of the coherent receiver (which includes the coherent receiver passive losses before the photodiodes), i_{TIA} is the input-referred noise current density of a single transimpedance amplifier, B_{eq}^{RX} is the effective noise bandwidth of the receiver, q is the electron charge and RIN is the LO RIN parameter. Finally, the SNR_Q parameter in Eq. (1) accounts for the additional implementation penalties associated with the power-independent effects occurring in a high-speed coherent system such as quantization noise, phase noise, imperfect constellation generation, etc. As a result of these distortion contributions, the BER curves as a function of the received optical power may exhibit an error floor at low BER values.

In Fig. 10, we superimpose the curves obtained through the analytical model on the back-to-back experimental curves shown in Fig. 5, in which the values of the four free parameters R, $CMRR$, i_{TIA} and SNR_Q) were obtained by a numerical fitting using a least mean square algorithm on the two experimental curves simultaneously. The resulting numerically fitted values are shown in Table I, and give an excellent agreement with both experimental BER sensitivity curves after the receiver DSP adaptive equalizer, and are also in line with the values reported in our commercial receiver

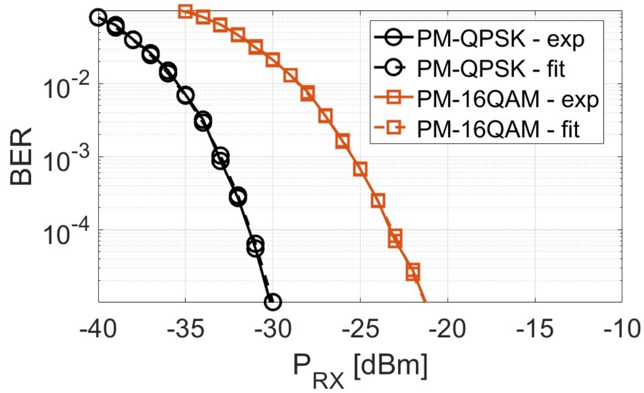

Fig. 10: BER vs. received signal power for the two modulation formats (PM-QPSK and PM-16QAM) at 28 $GBaud$. Solid lines: experiments. Dashed lines: analytical model.

datasheet. From the used laser datasheet we also inserted $RIN = -145\ dB/Hz$, while for the overall receiver noise bandwidth we set $B_{eq}^{RX} = 0.6 \cdot D$, where D is the system baud rate.

TABLE I: Model parameters extracted through fitting.

Parameter	Value	Unit
R	0.065	A/W
$CMRR$	-20	dB
i_{TIA}	19	pA/$\sqrt{Hz}$
SNR_Q	22.3	dB

B. Scalability Study Towards Higher Baud Rates

From our experimental characterization of the two-fiber self-coherent system, the sensitivity at SD-FEC BER=$2 \cdot 10^{-2}$ for PM-16QAM modulation is around -32 dBm (see Fig.7a), whereas the average power at the output of the modulator was in our experiments -6 dBm (considering that we have used commercial components and including the TX 1x2 splitter loss which we can conservatively set to 4 dB). Thus, we can reasonably estimate a very promising available power budget equal to 26 dB, that allows to envision extension of the proposed architecture to CWDM, since there is ample margin to cope with the additional loss of the required CWDM mux-demux filter, or even more exotic implementations in which in a ten-fiber MPO (five fibers for each direction) configuration, a 1x5 splitter is used at the transmitter, then four outputs are modulated, and the remaining one acts as a common local oscillator for four coherent receivers, thus reducing the impact of dedicating one fiber to the LO.

Taking advantage of the analytical model presented and validated in this Section [24]–[26], we are able to predict the performance of both the two-fiber and the ten-fiber MPO-based transmission schemes, in terms of the sensitivity margin defined as the difference between the received signal optical power and the sensitivity predicted by our model. This margin should be enough to ensure reliable operations considering additional penalties related to the practical implementation of the system, such as reduced DSP functionalities [8], [12] to minimize power consumption. We consider all the noise contributions described in previous Sections, although we do not assume any significant bandwidth limitation when we scale the baud rate up to higher values. The rationale here is to find ultimate scaling laws limited by intrinsic noises in an unamplified MPO-based self-coherent system, but not limited by opto-electronic components bandwidth. Also, as it is customary in IDC systems configurations, we do not consider any optical amplification.

A simplified schematic of the proposed two-fiber self-homodyne system employing a single transceiver is shown in Fig. 1.

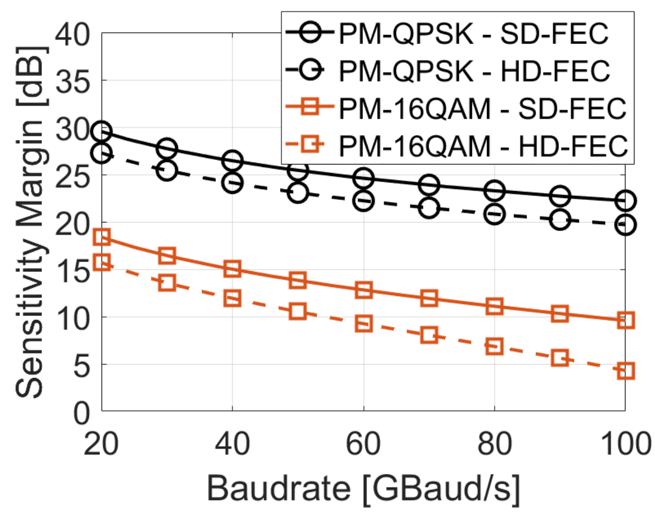

Fig. 11: Sensitivity margin as a function of the raw baud rate for the two modulation formats in a two-fiber MPO-based system. Solid lines: $BER = 2 \cdot 10^{-2}$ (SD-FEC). Dashed lines: $BER = 4 \cdot 10^{-3}$ (HD-FEC). The laser power is set to P_L^{CW}=16 dBm.

Fig. 11 shows the achievable sensitivity margin for the two considered modulation formats as a function of the raw bit rate at the two BER targets for the two-fiber system in Fig. 1, where we assume the same length for the two optical paths in the MPO. The laser power P_L^{CW} is set to 16 dBm, the LO power is about 4.5 dBm resulting from the 16 dBm transmitted power and the attenuation associated with the 1x2 splitter (4 dB), the 2.5 km fiber (0.5 dB), the polarization demultiplexing stage (3 dB [14]) and 4 dB of extra attenuation to take into account the losses associated with connectors and patch panels in a DC scenario. Notable margins above 9.5 dB and 22 dB can be observed, respectively for PM-QPSK and PM-16-QAM modulation for baud rates up to 100 $GBaud$ (400 $Gbps$ and 800 $Tbps$ gross total bit rates, respectively) at the SD-FEC BER threshold. With a HD-FEC the margin of the PM-QPSK-based system would be about 2.5 dB lower, whereas the PM-16QAM-based system would be limited to margins below 5 dB at 100 $GBaud$, primarily due to the BER floor in the sensitivity curves due to the SNR_Q parameter in Eq. (1) [7].

As an alternative and more advanced application of the self-coherent idea, we also studied the different architecture shown in Fig. 12, which reduces the percentage of fiber ”wasted” to carry tho local oscillator.

In the ten-fiber MPO system shown in Fig. 12, in both directions (five fibers downstream and five fibers upstream) a 1x5 optical splitter is used at the transmitter side to distribute the transmitted power over five different optical paths, four modulated and one CW signals. The unmodulated portion is then split again to serve as a LO for four different coherent receivers. In this case the LO undergoes some additional attenuation due to the extra splitting stage at the receiver. We estimate a total loss for the LO of about 22.5 dB resulting from the sum of 8 dB for the 1x5 splitter at the transmitter (including 1 dB insertion loss), 0.5 dB for 2.5 km fiber attenuation, 7 dB for the 1x4 splitter at the receiver, 3 dB for the optical polarization demultiplexing stage [14] and 4 dB of extra attenuation. Total loss for the modulated signals, including the modulator loss but not considering the loss due to the second splitting stage is about 26.3 dB and 30.7 dB for PM-QPSK and PM-16QAM modulation, respectively (we measured 13.8 and 18.2 dB modulator loss, respectively).

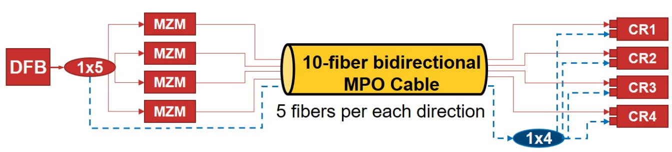

Fig. 12: Block diagram of the proposed MPO-based self-coherent system architecture. Only one transmission direction is shown. MZM: Mach Zender Modulator, CR: Coherent Receiver.

We show in Fig. 13 the achievable sensitivity margin for the two considered modulation formats as a function of the raw bit rate at the two BER targets, when the laser power P_L^{CW} is set to 16 dBm, the LO power is about -6.5 dBm (16 dBm transmitted minus 22.5 dB attenuation), and assuming the same length for the five optical paths.

Fig. 13 highlights that using 56 $GBaud$ PM-QPSK modulation a 224 $Gbps$ gross bitrate per lane (896 $Gbps$ total) can be easily achievable, leaving more than 10 dB of extra sensitivity margin, regardless of the considered FEC implementation.

56 $GBaud$ per lane (1.79 $Tbps$ gross total) would still be possible with PM-16QAM modulation coupled with a soft-FEC solution, but the sensitivity margin in this case would be reduced down to about 1 dB. Nevertheless, at 28 $GBaud$ (896 $Gbps$ gross total) even a system based on PM-16QAM modulation would have a non-negligible 4.5 dB sensitivity margin when equipped with soft-FEC technology.

V. Comments and Conclusion

In this paper, we focused on investigating if DFB lasers could be used as optical sources for next generation data center coherent links. We focus on the laser aspects since in today commercial coherent transceivers the (temperature controlled) ECL laser takes a great part of the overall transceiver cost. Replacing the ECL with a DFB, particularly in an uncooled

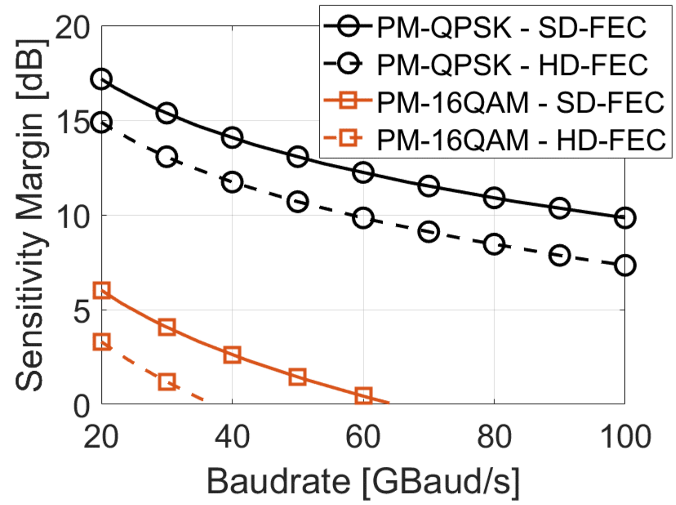

Fig. 13: Sensitivity margin as a function of the raw baud rate for the two modulation formats in a ten-fiber MPO-based system. Solid lines: $BER = 2 \cdot 10^{-2}$ (SD-FEC). Dashed lines: $BER = 4 \cdot 10^{-3}$ (HD-FEC). The laser power is set to P_L^{CW}=16 dBm.

version would significantly reduce the cost. To this end, we have experimentally evaluated the effect of the laser phase noise in a self-coherent transmission system for IDC applications, studying how the beating linewidth increases with the optical path difference between the signal and the remotely generated local oscillator. We showed that when 28 $GBaud$ PM-QPSK and PM-16QAM modulation formats are used the phase noise-induced sensitivity penalty reaches 1 dB when the path difference between the signal and the LO is 1.8 m and 0.8 m, respectively at the SD-FEC threshold. We also found that the penalty is equivalent in B2B and for transmission over a 2.5 km SMF fiber. Our results prove that the use of DFB lasers in the proposed system is possible, even for PM-16QAM up to fiber path difference of less than about 0.8 meters, a requirement that seems not critical for instance in multi-parallel optic cables, where the two fibers would have almost identical length, since they would run in the same MPO. Identical transceivers can be deployed at both ends of the communication system, with a potential for further simplification and cost reduction associated with the use of uncooled DFB laser [13] and all-optical polarization tracking device to compensate for random polarization rotation effects on the LO path [14].

In order to obtain scalability trends for MPO-based self-coherent systems, we have also studied the performance of a self-coherent transmission system through an analytical model, extracting the main model parameters through fitting of the experimental back-to-back sensitivity curves. The analytical tool can predict the performance of our experimental 28 $Gbaud$ PM-QPSK and PM-16QAM system with remarkable accuracy based on a realistic set of extracted parameters. The model has then been used to investigate the possibility of using a 10-fiber MPO cable to share the same remotely generated local oscillator among four transmission lanes. The scaling laws describing the system performance at very high aggregate gross bit rates highlight the feasibility of such a system, yielding over 10 dB and about 4 dB sensitivity margin, respectively for PM-QPSK and PM-16QAM modulation at 896 $Gbps$ per lane.

In conclusion, we can summarize the pros and cons of the proposed solution as follows:

- Pros
  - Use of DFB lasers (possibly in the uncooled version) instead of ECL.
  - Partially simplified DSP since laser alignment is not needed.
- Cons
  - One fiber dedicated to the LO.
  - Need for a polarization tracker on the LO of the coherent receiver.

Acknowledgment

This work was carried out under the PhotoNext initiative at Politecnico di Torino (http://www.photonext.polito.it).

References

[1] G. Rademacher, R. S. Lus, B. J. Puttnam, R. Ryf, S. van der Heide, T. A. Eriksson, N. K. Fontaine, H. Chen, R. Essiambre, Y. Awaji, H. Furukawa, and N. Wada, “172 Tb/s C+L Band Transmission over 2040 km Strongly Coupled 3-Core Fiber,” in *Proc. OFC*, San Diego, CA, USA, 2020, paper Th4C.5.

[2] F. Buchali, V. Aref, M. Chagnon, K. Schuh, H. Hettrich, A. Bielik, L. Altenhain, M. Guntermann, R. Schmid, and M. Moller, “1.52 Tb/s single carrier transmission supported by a 128 GSa/s SiGe DAC,” in *Proc. OFC*, San Diego, CA, USA, 2020, paper Th4C.2.

[3] Xiaodan Pang, Oskars Ozolins, Rui Lin, Lu Zhang, Aleksejs Udalcovs, Lei Xue, Richard Schatz, Urban Westergren, Shilin Xiao, Weisheng Hu, Gunnar Jacobsen, Sergei Popov, and Jiajia Chen, “200 Gbps/Lane IM/DD Technologies for Short Reach Optical Interconnects,” in *Journal of Lightwave Technology*, vol. 38, no. 2, pp. 492-503, Jan. 2020.

[4] X. Zhou, R. Urata and H. Liu, “Beyond 1 Tb/s Intra-Data Center Interconnect Technology: IM-DD OR Coherent?,” in *Journal of Lightwave Technology*, vol. 38, no. 2, pp. 475-484, Jan. 2020.

[5] The Optical Internetworking Forum, “Flex Coherent DWDM Transmission Framework Document,” (2017) [Online].

[6] G. Rizzelli and R. Gaudino, “Sensitivity and Scaling Laws of Unamplified Coherent Architectures for Intra-Data Center Links Beyond 100 Gb/s,” in *Proc. ICTON*, Angers, France, 2019, pp. 1-4.

[7] G. Rizzelli Martella, A. Nespola, S. Straullu, F. Forghieri and R. Gaudino, “Scaling Laws for Unamplified Coherent Transmission in Next-Generation Short-Reach and Access Networks,” in *Journal of Lightwave Technology*, vol. 39, no. 18, pp. 5805-5814, Sept. 2021.

[8] M. Morsy-Osman, M. Sowailem, E. El-Fiky, T. Goodwill, T. Hoang, S. Lessard and D. V. Plant, “Design of Low-Power DSP-Free Coherent Receivers for Data Center Links,” in *Journal of Lightwave Technology*, vol. 35, no. 21, pp. 4650-4662, Nov. 2017.

[9] M. Chagnon, “Optical Communications for Short Reach,” in *Proc. ECOC*, Rome, Italy, 2018, pp. 1-3.

[10] H. Ji, X. Zhou, C. Sun and W. Shieh, “Polarization-diversity receiver using remotely delivered local oscillator without optical polarization control”, in *Optics Express*, vol.28, no. 15, pp. 22882-22890, 2020.

[11] Honglin Ji, Xian Zhou, Chuanbowen Sun, and William Shieh, “Theoretical Analysis of Phase Noise Induced by Laser Linewidth and Mismatch Length in Self-Homodyne Coherent Systems,” in *J. Lightwave Technol.*, vol. 39,no. 5, pp. 1312-1321, March 2021.

[12] J. K. Perin, A. Shastri and J. M. Kahn, “DSP-free coherent-lite transceiver for next generation single wavelength optical intra-datacenter interconnects,” in *Optics Express*, vol.26, no. 7, pp. 8890-8903, 2018.

[13] T. Gui, X. Wang, M. Tang, Y. Yu, Y. Lu, and L. Li, “Real-Time Demonstration of 600 Gb/s DP-64QAM SelfHomodyne Coherent Bi-Direction Transmission with Un-Cooled DFB Laser,” in *Proc. OFC*, San Diego, CA, USA, 2020, paper Th4C.3.

[14] A. Nespola et al., “Proof of Concept of Polarization-Multiplexed PAM Using a Compact Si-Ph Device,” in *Photonic Technology Letters*, vol. 31, no. 1, pp. 62-65, Jan. 2019.

[15] Li Wang, Yifan Zeng, Ting Yang, Chao Xin, Haoze Du, Xuefeng Wang, Ming Tang. (2021, September). First Real-time MIMO-free 800Gb/s DP-64QAM Demonstration Using Bi-Directional Self-homodyne Coherent Transceivers. Presented at ECOC 2021. [Online]. Available: https://www.ecoc2021.org/programme/post-deadline-papers.

[16] G. Rizzelli, A. Nespola, S. Straullu, F. Forghieri and R. Gaudino, “Two-Fiber Self-Homodyne Transmission for Short-Reach Coherent Optical Communications,” in *Proc. ICTON*, Bari, Italy, 2020, pp. 1-4.

[17] K. Kikuchi and K. Igarashi, “Characterization of Semiconductor-Laser Phase Noise with Digital Coherent Receivers,” in *Proc. OFC/NFOEC*, Los Angeles, CA, USA, 2012, paper OML3.

[18] L. B. Mercer, “1/f frequency noise effects on self-heterodyne linewidth measurements,” in *Journal of Lightwave Technology*, vol. 9 ,no. 4, pp. 485-493, Apr. 1991.

[19] M. G. Taylor, “Phase Estimation Methods for Optical Coherent Detection Using Digital Signal Processing,” in *Journal of Lightwave Technology*, vol. 27, no.7, pp. 901–914, Apr. 2009.

[20] N. Argyris, S. Dris, C. Spatharakis and H. Avramopoulos, “High performance carrier phase recovery for coherent optical QAM,” in *Proc. OFC*, Los Angeles, CA, USA, 2015, paper W1E.1.

[21] J. H. Ke, K. P. Zhong, Y. Gao, J. C. Cartledge, A. S. Karar and M. A. Rezania, “Linewidth-Tolerant and Low-Complexity Two-Stage Carrier Phase Estimation for Dual-Polarization 16-QAM Coherent Optical Fiber Communications,” in *Journal of Lightwave Technology*, vol. 30, no.24, pp. 3987-3992, Dec. 2012.

[22] S. J. Savory, “Digital Coherent Optical Receivers: Algorithms and Subsystems,” in *Journal of Selected Topics in Quantum Electronics*, vol. 16, no. 5, pp. 1164-1179, Sept.-Oct. 2010.

[23] R. Gaudino, V. Curri, G. Bosco, G. Rizzelli, A. Nespola, D. Zeolla, S. Straullu, S. Capriata, and P. Solina, “On the use of DFB Lasers for Coherent PON,” in *Proc. OFC*, Los Angeles, CA, USA, 2012, paper OTh4G.1.

[24] B. Zhang, C. Malouin, and T. Schmidt, “Design of coherent receiver optical front end for unamplified applications,” in *Optics Express*, vol. 20, no. 3, pp. 3225-3234, 2012.

[25] K. Kikuchi, and S. Tsukamoto, “Evaluation of Sensitivity of the Digital Coherent Receiver,” in *Journal of Lightwave Technology*, vol. 26 no. 13, pp. 1817-1822, Jul. 2008.

[26] D. Lavery, S. Liu, Y. Jeong, J. Nilsson, P. Petropoulos, P. Bayvel, and S. Savory, “Realizing High Sensitivity at 40 Gbit/s and 100 Gbit/s,” in *Proc. OFC*, Los Angeles, CA, USA, 2012, paper OW3H.5.